

Self-assembled InGaN quantum dots on GaN emitting at 520 nm grown by metalorganic vapor-phase epitaxy

Yik-Khoon Ee*, Hongping Zhao, Ronald A. Arif, Muhammad Jamil, Nelson Tansu

Department of Electrical and Computer Engineering, Center for Optical Technologies, Lehigh University, Bethlehem, PA 18015, USA

Available online 31 January 2008

Abstract

Self-assembled InGaN quantum dots (QDs) have been grown using metalorganic vapor-phase epitaxy (MOVPE), without using anti-surfactant. Using 120 s annealing, InGaN QDs have been successfully formed with a circular base diameter of 40 nm and an average height of 4 nm, with QDs density of $4 \times 10^9 \text{ cm}^{-2}$. The InGaN QDs have peak photoluminescence (PL) wavelengths of 519 and 509 nm for samples without and with a GaN upper barrier, respectively. The full-width half-maximum (FWHM) of the PL spectra ranges from 56.6 up to 69.6 nm. These results demonstrate that high In-content InGaN QDs can be grown by MOVPE, and can potentially be utilized as the active media for light-emitting diodes (LEDs) and semiconductor laser diodes for green emission.

© 2008 Elsevier B.V. All rights reserved.

PACS: 68.37.Ps; 68.65.Hb; 73.61.Ey; 78.67.-n; 81.16.Dn; 82.33.Ya; 85.60.Jb

Keywords: A1. Low-dimensional structures; A1. Nanostructures; A3. Metalorganic chemical vapor deposition; B1. Nitrides; B2. Semiconducting III–V materials

1. Introduction

The current commercial approach for achieving white-light solid-state sources is by using blue or ultraviolet InGaN quantum wells (QW) light-emitting diodes (LEDs) to excite the yellow-green and red phosphors, thus resulting in broadband visible white emission in the blue–green–yellow–red regions [1]. However, this approach suffers reduced quantum efficiency due to the limited external quantum efficiency of the wavelength conversion in phosphors materials, and intrinsic quantum mechanical energy loss of the wavelength conversion process via Stokes shift.

The most energy-efficient approach for generating white-light sources is to generate the blue, green, and red light sources via independent LEDs. The use of monolithically integrated nitride-based blue–green–red LEDs will result in energy-efficient and low-cost approach for the white-light LEDs. This monolithic technique requires high-efficiency

nitride-based LEDs emitting in green and red regions, for implementation with blue InGaN QW LEDs for high-efficiency solid-state lighting applications. While InGaN QW LEDs emitting in the blue region has been realized with acceptable performances, high-efficiency green LEDs utilizing the same QW materials have proven to be more challenging. Group III-nitride LEDs emitting in the green region ($\lambda \sim 520\text{--}540 \text{ nm}$) can be achieved by increasing the In-content in the $\text{In}_x\text{Ga}_{1-x}\text{N}$ QW to $\sim 24\%$ (with thickness of $\sim 25 \text{ \AA}$), but the high strain in the QW leads to strain relaxation via misfit defect formation resulting in increased dislocation density, and phase separation with In mole fraction inhomogeneity in the InGaN QW [1].

In this work, we investigate the metalorganic vapor-phase epitaxy (MOVPE) epitaxy of self-assembled InGaN quantum dots (QDs), emitting in the 510–520 nm region (green emission). The ability to grow high-quality InGaN-active region with high In-content (In $> \sim 25\text{--}40\%$) with minimum strain-induced misfit defect formation is crucial for achieving high-efficiency nitride-based LEDs emitting in the green ($\lambda \sim 510 \text{ nm}$) region or beyond ($\lambda \sim 650 \text{ nm}$). The advantage of the QDs implementation into the laser-active

*Corresponding author. Tel.: +1 610 758 4326; fax: +1 610 758 2605.

E-mail addresses: Ee@Lehigh.Edu (Y.-K. Ee), Tansu@Lehigh.Edu (N. Tansu).

regions also include low-transparency carrier and current density, reduced temperature sensitivity, and reduced threshold current density of the diode lasers.

2. Self-assembled InGaN quantum dots

In contrast to the studies done on InGaAs-based QDs on GaAs [2–5], only very few preliminary works have been conducted on the epitaxy of InGaN QDs on GaN. Several approaches have been investigated for growing self-assembled InGaN QDs, including Stranski–Krastanow growth mode [6–13], growth using Si-based anti-surfactant [14], droplet epitaxy [15], and post-growth anneal approach [16]. All the prior works on the self-assembled InGaN QDs by MOVPE had been conducted with low In-content for blue emission ($\lambda \sim 420\text{--}465\text{ nm}$) [2–10], and blue-green region ($\lambda \sim 475\text{--}495\text{ nm}$) [11]. Previously, molecular beam epitaxy (MBE)-grown InGaN QDs had been demonstrated with emission in the blue-green region (477–529 nm) [17].

In the growth of InGaN QDs, a very thin strained layer with thickness of 6–8 monolayers (MLs) of InGaN material is epitaxially deposited on the GaN barrier layer resulting in the surface strain energy built up. The growth rate of the thin strained layer is kept high, thus allowing a 2D thin strained layer deposition with thickness of 6–8 MLs as shown schematically in Fig. 1(a). By implementing an in-situ thermal annealing of the 2D thin strained layers under N_2 gas (without groups V and III gas sources), this allows atomic re-arrangements on the thin strained layer surface resulting in the lowest surface strain energy atomic configurations as shown in Fig. 1(b). Once the self-assembled InGaN QDs were formed, the epitaxy of the GaN upper barrier can be conducted as shown in Fig. 1(c). It is very important to distinguish the atomic arrangement for InGaN QDs, and the strain relaxation for the high In-content InGaN QWs. For the case of QWs, the strain relaxation releases the surface strain energy via the creation of misfit defect dislocation. In contrast to the case of QWs, the atomic reordering during N_2 annealing allows the release of strain energy of the layer by increasing the surface area via the re-arrangement of the atoms into defect-free 3D QDs nanostructures and wetting layer, prior to the growth of subsequent layers (i.e. GaN upper barrier). In this paper, we focus on the studies of the epitaxial growth conditions and optical properties of

MOVPE-grown self-assembled InGaN QDs, emitting in the 520 nm region (green emission) without using anti-surfactant.

3. Experimental procedure

All the InGaN QDs samples used in this study were grown using a vertical-type VEECO P-75 MOVPE reactor. The gallium, indium and nitrogen precursors used were trimethylgallium (TMGa), trimethylindium (TMIn) and ammonia (NH_3), respectively. In our studies, the growths of InGaN QDs were conducted on the undoped-GaN (u-GaN) template grown on *c*-plane sapphire substrates.

The growth of $3\text{ }\mu\text{m}$ u-GaN template on the *c*-plane sapphire was performed at a temperature of $1080\text{ }^\circ\text{C}$, employing a low-temperature 30-nm-thick u-GaN nucleation layer at $535\text{ }^\circ\text{C}$. During the growth of the u-GaN template layer, the H_2 carrier gas flow was 3000 sccm, the molar flow rate of TMGa was $10\text{ }\mu\text{mol}/\text{min}$ and NH_3 was used as group V source with a flow rate of 2500 sccm, corresponding to a V/III ratio of 1815.

In our QDs experiments, both the InGaN QDs and barrier regions were grown at low temperature ($T_g = 660\text{ }^\circ\text{C}$) on the u-GaN template. The low-temperature growth is designed for allowing higher In-content incorporation as well as allowing the growth of highly-strained materials with less relaxation. Prior to the growth of both QDs and barriers at a temperature of $660\text{ }^\circ\text{C}$, a thin $0.3\text{ }\mu\text{m}$ high-temperature u-GaN ($1080\text{ }^\circ\text{C}$) was grown on the u-GaN/sapphire template. For the growth of the 12-nm-thick u-GaN lower barrier, we employed triethylgallium (TEGa) as the Ga-precursor with TEGa molar flow rate and V/III ratio of $0.68\text{ }\mu\text{mol}/\text{min}$ and 18,900, respectively. The 2D InGaN layer with different thicknesses ranging from 6 up to 12 MLs was then grown on the u-GaN lower barrier. The carrier gas was switched to N_2 and the flow rate was 2500 sccm. The NH_3 flow rate was increased to 5000 sccm, corresponding to a V/III molar ratio of 7500 for the 2D InGaN growth. The growth of the 2D InGaN layer is followed by annealing of 120 s under N_2 at $660\text{ }^\circ\text{C}$ without Groups III and V species. The time evolutions of the growth temperature and reflectivity profiles for the QDs and barriers growths are shown in Fig. 2. In Fig. 2, the temperature and reflectivity profiles are shown for (1) the growth of the 2D InGaN

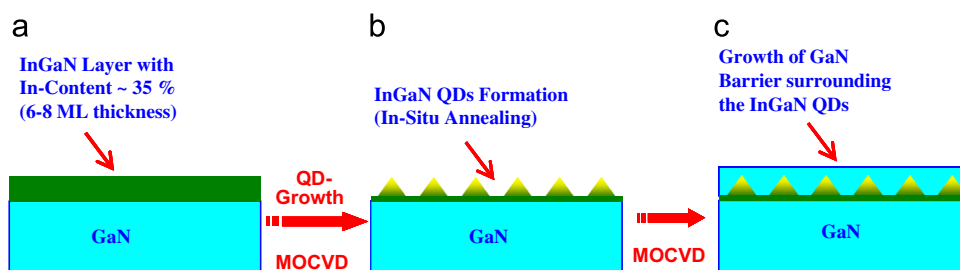


Fig. 1. Schematic representation of self-assembled InGaN QDs growth by MOVPE, with (a) InGaN 2D layer growth, (b) QD formation annealing process, and (c) growth of upper GaN barriers.

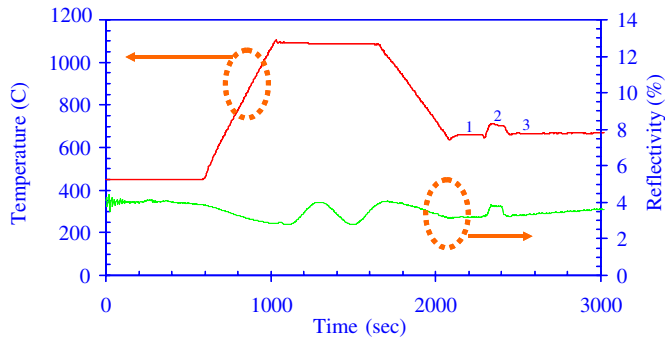


Fig. 2. The growth temperature and reflectivity profiles for the InGaN QDs growth. Stage (1) shows the stage of the 2D InGaN layer growth, (2) shows the growth of InGaN QDs with N_2 annealing, and (3) shows the growth of a 12 nm undoped GaN upper barrier layer.

layer, (2) 120 s N_2 thermal annealing stage for the growth of InGaN QDs, and (3) growth of 12 nm u-GaN upper barrier using TEGa precursor.

The flow rates of TMGa and TMIIn for the growth of 2D InGaN layer were 2.46 and 2.40 $\mu\text{mol}/\text{min}$, respectively. The In-content in the 2D InGaN epilayer is estimated as 35% from X-ray diffraction measurement and growth calibration. During the N_2 thermal annealing stage (without Groups III and V source) for the formation of the 3D InGaN QDs, there would be material loss due to the indium evaporation. Thus, the In-content for the InGaN QDs is expected to be lower due to the indium evaporation. From our studies, we found that the InGaN QDs formation was very sensitive to the surface morphology of the u-GaN lower barrier. To investigate the effect of the template surface on the formation of InGaN QDs, we investigate two different u-GaN lower barrier layer as follows: (1) grown using TEGa as the Ga-precursor, and (2) grown using TMGa as the Ga-precursors, prior to the growth of 2D InGaN layer. The surface morphologies of these samples were characterized by an atomic force microscopy (AFM) system (Digital Instruments Nanoscope Dimension 3000) with a sharpened Si_3N_4 tip at room temperature. Photoluminescence (PL) was also used to study the optical properties of the InGaN QDs, using the He–Cd laser with wavelength at 325 nm as the excitation source at room temperature.

4. Results and discussions

The initial QDs growths were conducted on the GaN barrier layers grown using TEGa precursor, as shown in Fig. 3(a) and (b). Fig. 3(a) and (b) show the $1 \times 1 \mu\text{m}^2$ AFM images of the 10 and 12 MLs thick InGaN epilayer after undergoing the in-situ annealing. As shown in the surface morphology of these figures, large dimension (100–200 nm dimensions) incoherent 3D nanostructures with the random size and shape distribution were formed after the annealing process. This process is very different from the annealing process resulting in the formation of self-assembled coherent QDs with narrow size distribution

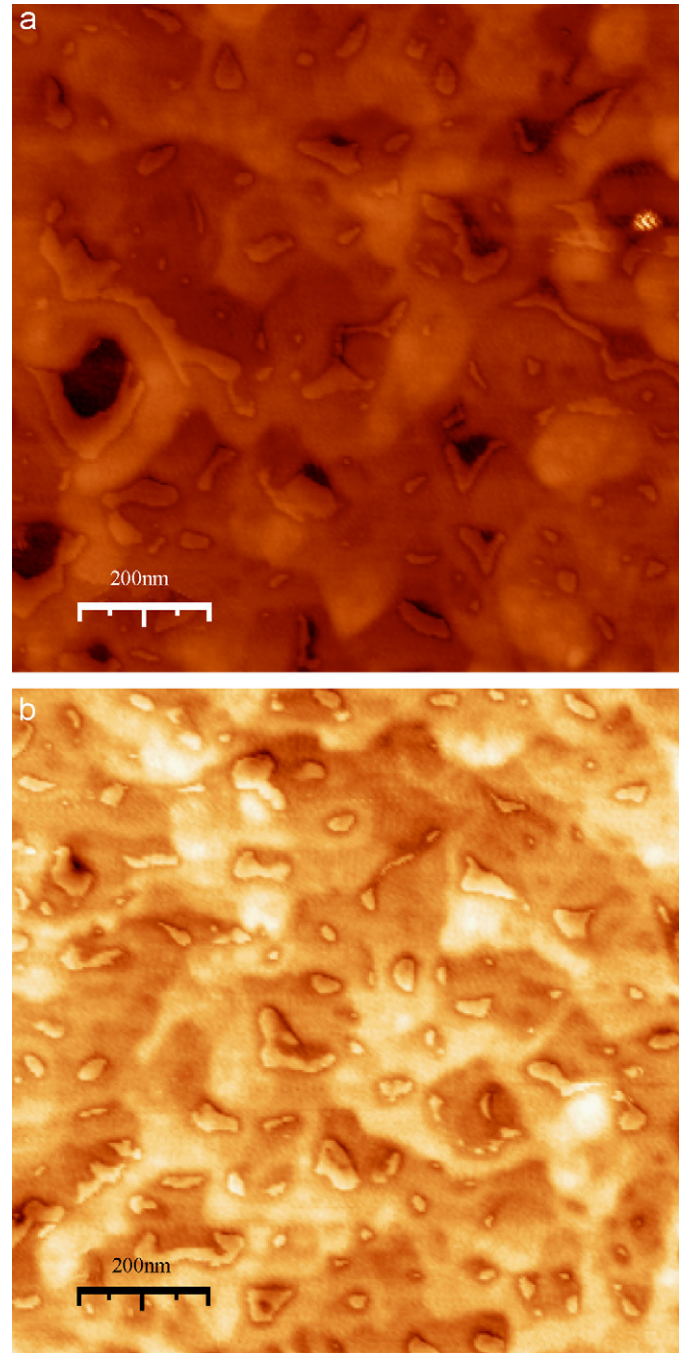


Fig. 3. AFM micrograph of (a) 10 MLs and (b) 12 MLs of InGaN epilayer after 120 s in-situ annealing in N_2 , with GaN lower barrier grown using TEGa precursor.

and regular shapes. It is important to note that the QD growth is a strain-driven process, and the formation of large incoherent 3D nanostructures could be attributed to either (1) a thickness of 2D InGaN epilayer much higher than the critical layer thickness, or/and (2) rough GaN template.

To study the effect of the 2D InGaN thickness on the 3D nanostructures formation, the thickness of the 2D InGaN epilayer was reduced to 7 and 8 MLs on the GaN barrier layer grown using TEGa precursor, and the AFM images

are shown in Fig. 4(a) and (b) respectively. The AFM images of the InGaN layer with the reduced thickness also show that the layer did not form the coherent QDs, rather the annealing process resulted in the nano-holes with diameters of 50–75 nm and depth dimensions in the range of 1.5–2.5 nm. The observed nano-holes patterns in InGaN occur due to the thickness of the 2D InGaN epilayer exceeding the critical thickness. Part of the strain in InGaN epilayer was reduced elastically by the formation of nano-holes, similar to those observed in the case of InGaAs [18].

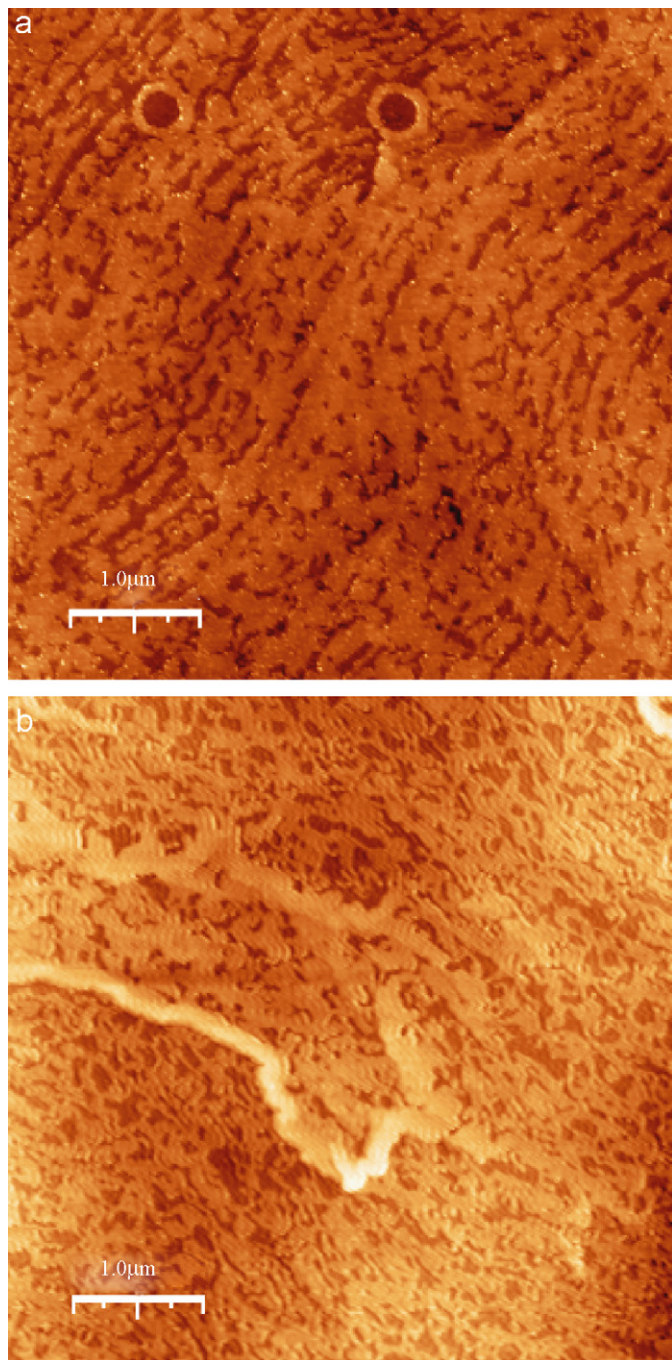


Fig. 4. AFM micrograph of (a) 7 MLs and (b) 8 MLs of InGaN epilayer after 120 s in-situ annealing in N_2 , with GaN lower barrier grown using TEGa precursor.

Note that both the samples exhibited two types of distinctly different incoherent nanostructures. For the 10 and 12 MLs thick InGaN epilayer, large incoherent 3D nanostructures were formed after annealing. For the 7 and 8 MLs thick InGaN epilayer, nano-holes were formed after annealing.

Experiments were then conducted to investigate the surface morphology of the template before the growth of the 2D InGaN epilayer. AFM analysis was done on the GaN barrier layer prior to the growth of 2D InGaN,

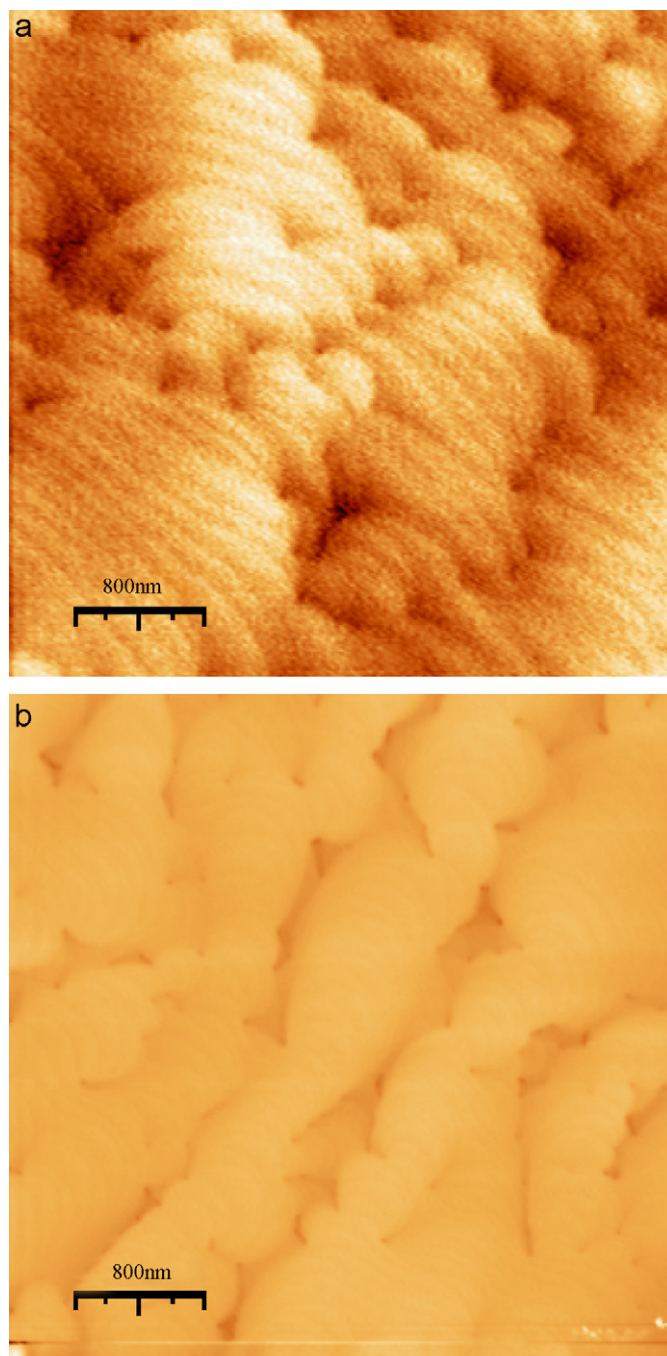


Fig. 5. AFM micrograph comparison of GaN lower barrier grown using (a) TMGa and (b) TEGa as Ga-precursor. The RMS roughness of the GaN barriers are 0.30 and 0.61 nm, respectively.

grown using TMGa and TEGa precursor as shown in Fig. 5(a) and (b), respectively. The surface of the GaN barrier grown using TMGa precursor (V/III ratio = 14,600) indicates smooth atomic-step morphology with RMS roughness of about 0.30 nm. The AFM of the GaN barrier grown using TEGa precursor indicated a RMS roughness of 0.61 nm, which was twice the roughness of that grown with TMGa precursor, which was also observed by Song and co-workers [19].

A series of growth experiments were then conducted using GaN barrier grown using TMGa precursor. Experiment was then conducted by growing 6 MLs of 2D InGaN epilayer, followed by 120 s annealing under N₂ environment. Fig. 6 shows the AFM image of the coherent self-assembled InGaN QDs formation. The N₂ annealing of the InGaN thin film results in the QD formation with circular base diameter of ~40 nm and height of ~4 nm, as shown in the inset of Fig. 6. The InGaN QDs density is estimated as $4 \times 10^9 \text{ cm}^{-2}$. The desired QDs density for high-performance emitter devices typically requires $\sim 2\text{--}4 \times 10^{10} \text{ cm}^{-2}$. The low-InGaN QDs density ($4 \times 10^9 \text{ cm}^{-2}$) from our experiments can be presumably attributed to the larger QDs dimensions, as well as material loss during N₂ annealing thus reducing its density.

We have also conducted AFM imaging on the 2D InGaN layer with and without N₂ annealing stage, and we found that the InGaN QDs were formed only after undergoing the N₂ thermal annealing. From our experimental studies, we found that the formation of InGaN QDs was very sensitive to the surface morphology of the lower GaN barrier. The low RMS roughness of the surface template prior to the QD growth is important for allowing the 3D formation of the coherent InGaN QDs. From our

studies with TMGa-based GaN barrier, we also found that the use of InGaN epilayer exceeding 10 MLs also resulted in incoherent 3D nanostructures after the annealing process. This indicates that the growth of the coherent InGaN QDs without the use of anti-surfactant is very sensitive to (1) composition and thickness of 2D InGaN epilayer, (2) critical thickness limitation of 2D InGaN epilayer (for 2D In_{0.35}Ga_{0.65}N the critical thickness limit is approximately 7–8 MLs [20]), and (3) surface morphology and material quality of the u-GaN barrier material prior to the QD growth.

PL measurements were conducted on the samples consisting of active regions of a single layer of InGaN QDs. For comparison purpose, the PL measurements were conducted on the samples with and without GaN upper barrier cap layer. The He–Cd laser ($\lambda = 325 \text{ nm}$) was used as the excitation source from the backside of the samples at room temperature. The PL was collected from the top surface of the samples. Fig. 7 shows the PL spectra of the MOVPE-grown InGaN QDs PL samples with and without GaN upper barrier layer. The PL peak luminescence wavelengths (λ_{peak}) for the QD samples with and without GaN upper barrier cap layer are measured as 509 and 519 nm, emitting in the green regions. The relatively broad full-width-half-maximum (FWHM) of the PL spectra for both the samples range from 56.6 up to 69.6 nm. For comparison purpose, the peak and integrated PL intensities of the single layer InGaN QDs are 22.7% and 40.4% of that of a four-period multiple 3 nm In_{0.25}Ga_{0.75}N QW quantum well ($\lambda \sim 538 \text{ nm}$). The broadened PL spectrum is attributed to the inhomogeneous size distribution of the InGaN QDs, as well as varying indium composition in each dot. Hence, the transition levels of these dots are

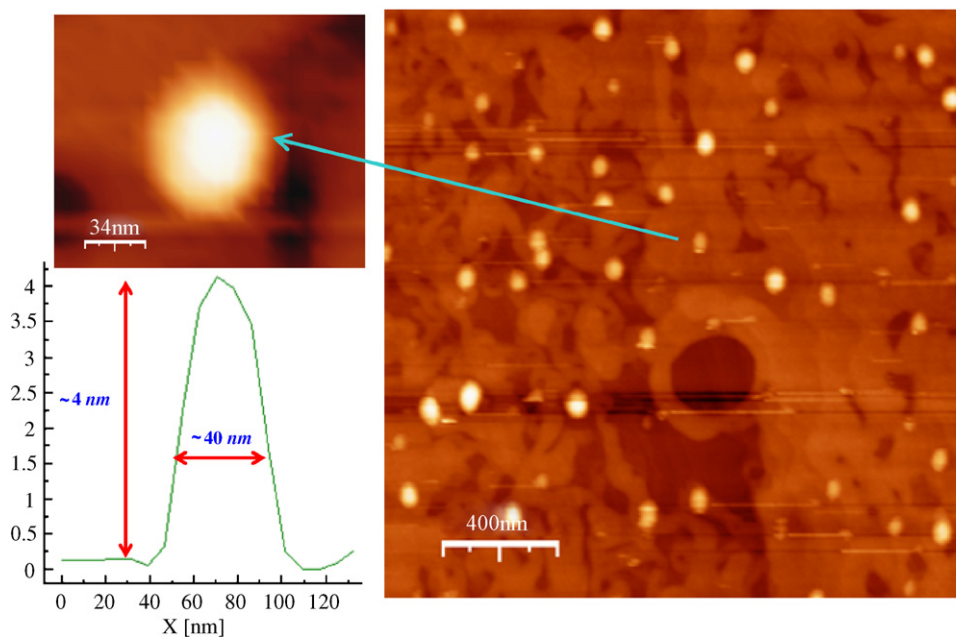


Fig. 6. AFM image of MOVPE-grown self-assembled InGaN QDs, employing annealing time of 120 s. The inset shows a representative of the InGaN QD with circular base diameter of ~40 nm and height of ~4 nm. The InGaN QD density is measured as $4 \times 10^9 \text{ cm}^{-2}$.

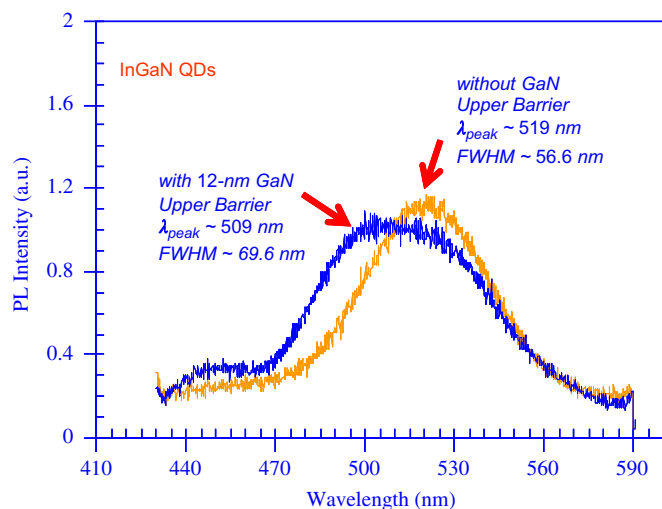


Fig. 7. Photoluminescence spectra of InGaN QDs samples with and without the upper GaN barrier layer, with λ_{peak} of 509 and 519 nm, respectively.

different from one another, thereby broadening the PL spectrum. Future work include the optimization of the QD density and its size distribution by optimizing the growth conditions for LEDs device implementation.

5. Summary

In conclusion, the MOVPE epitaxy of self-assembled InGaN QDs emitting at ~ 520 nm on GaN were reported. From the AFM studies, the density and dimensions of the InGaN QDs were measured as $\sim 4 \times 10^9 \text{ cm}^{-2}$, and circular base diameter of ~ 40 nm and height of ~ 4 nm, respectively. Our works also indicated that the MOVPE growth of coherent InGaN QDs depends critically on the (1) critical thickness limitation of the InGaN layer, and (2) surface morphology of the GaN barrier prior to the QD growth. PL measurements of InGaN QDs indicated λ_{peak} of ~ 520 nm, with inhomogeneously broadened FWHM of 56.6–69.6 nm. These results demonstrated InGaN QDs with high In-content can be grown by MOVPE, and the use of QDs can be potentially implemented as the active medium in the high efficiency green LEDs, as well as delivering low threshold green semiconductor lasers.

Acknowledgments

The authors would like to acknowledge funding support from US Department of Defense—Army Research Lab, National Science Foundation (NSF) Award #0701421, and P.C. Rossin Assistant Professorship Funds.

References

- [1] S. Nakamura, *Science* 281 (1998) 956.
- [2] F. Heinrichsdorff, A. Krost, D. Bimberg, A.O. Kosogov, P. Werner, *Appl. Surf. Sci.* 123 (1998) 725.
- [3] R.L. Sellin, I. Kaiander, D. Ouyang, T. Kettler, U.W. Pohl, D. Bimberg, N.D. Zakharov, P. Werner, *Appl. Phys. Lett.* 82 (2003) 841.
- [4] D. Bimberg, N. Kirstaedter, N.N. Ledentsov, Zh.I. Alferov, P.S. Kop'ev, V.M. Ustinov, *IEEE J. Select. Top. Quant. Electron.* 3 (1997) 196.
- [5] K. Mukai, Y. Nakata, K. Otsubo, M. Sugawara, N. Yokoyama, H. Ishikawa, *IEEE Photon. Technol. Lett.* 11 (1999) 1205.
- [6] K. Tachibana, T. Someya, Y. Arakawa, *Appl. Phys. Lett.* 74 (1999) 383.
- [7] O. Moriwaki, T. Someya, K. Tachibana, S. Ishida, Y. Arakawa, *Appl. Phys. Lett.* 76 (2000) 2361.
- [8] L.W. Ji, T.H. Fang, T.H. Meen, *Phys. Lett. A* 355 (2006) 118.
- [9] J. Ou, W.K. Chen, H.C. Lin, Y.C. Pan, M.C. Lee, *Jpn. J. Appl. Phys.* 37 (1998) L633.
- [10] S. Ruffenach, B. Maleyre, O. Briot, B. Gil, *Phys. Stat. Sol. C* 2 (2005) 826.
- [11] H.H. Yao, T.C. Lu, G.S. Huang, C.Y. Chen, W.D. Liang, H.C. Kuo, S.C. Wang, *Nanotechnology* 17 (2006) 1713.
- [12] H.J. Kim, H. Na, S.Y. Kwon, H.C. Seo, H.J. Kim, Y. Shin, K.H. Lee, D.H. Kim, H.J. Oh, S. Yoon, C. Sone, Y. Park, E. Yoon, *J. Crystal Growth* 269 (2004) 95.
- [13] L.W. Ji, Y.K. Su, S.J. Chang, L.W. Wu, T.H. Fang, J.F. Chen, T.Y. Tsai, Q.K. Xue, S.C. Chen, *J. Crystal Growth* 249 (2003) 144.
- [14] T.C. Wang, H.C. Kuo, T.C. Lu, C.E. Tsai, M.Y. Tsai, J.T. Hsu, J.R. Yang, *Jpn. J. Appl. Phys.* 45 (2006) 3560.
- [15] J.H. Rice, R.A. Oliver, J.W. Robinson, J.D. Smith, R.A. Taylor, G.A.D. Briggs, M.J. Kappers, C.J. Humphreys, S. Yasin, *Physica E* 21 (2004) 546.
- [16] R.A. Oliver, G.A.D. Briggs, M.J. Kappers, C.J. Humphreys, S. Yasin, J.H. Rice, J.D. Smith, R.A. Taylor, *Appl. Phys. Lett.* 83 (2003) 755.
- [17] B. Damilano, N. Grandjean, S. Dalmaso, J. Massies, *Appl. Phys. Lett.* 75 (1999) 3751.
- [18] J.J. Russell-Harriott, A.R. Moon, J. Zou, D.J.H. Cockayne, B.F. Usher, *IEEE Opt. Micro. Mater. Dev. Proc.* 287 (1998).
- [19] K. Song, D. Kim, Y. Moon, S. Park, *J. Crystal Growth* 233 (2001) 439.
- [20] B. Jahnen, M. Albrecht, W. Dorsch, S. Christiansen, H.P. Strunk, D. Hanser, R.F. Davis, *MRS J. Nitride Semicond. Res.* 3 (1998) 39.